Development of continuous slab casting technology with dimensions of (300–400) mm × (2000–2500) mm OF high-alloy martensitic steel

A. V. Kuklev · V. V. Tinyakov · A. V. Ermolaev · C. Zamboni · E. Donskoi

Received: 5 April 2023 / Revised: 15 May 2023 / Accepted: 20 October 2023 / Published online: 15 May 2024

Abstract
This study discusses the problem of continuous casting of high-alloy, martensitic steel into a (300–400) mm × (2000–2500) mm slabs for production of a 70–100 mm thick sheet. At the beginning of the technology development, the specialists encounter the formation of a considerable number of surface defects in the slabs, such as "scabs," "longitudinal cracks along the scabs," and "flash." The causes of the defects are determined during the course of this study. The shrinkage in the steel sample is measured, and that in the ingot crust in the casting mold is calculated. A new mold setting (tapering) is developed. The submerged nozzle design and slag-forming mixture composition for the mold are optimized. A new polynomial for calculating the liquidus temperature of high-carbon, high-chromium steels is developed and tested in practice. The use of the developed algorithm enabled to optimize the overheating of the steel.
The application of the technology developed has considerably enhanced the quality of the slabs.

Keywords Continuous casting · Mold · Slag-forming mixture · Ingot · Surface "scab" defects

Molds are used for pressing large plastic products worldwide; these are made from thick, rolled plates of high-alloy, wear-resistant, martensitic chromium-molybdenum steel type W 1.2085 (X33Cr16 + S). The composition of this steel type is presented in Table 1.

Previously, thick slabs of this steel were produced via smelting in an arc furnace, processing in a ladle furnace installation, evacuation in a ladle refining installation, casting into a mold, heating of the ingot in a bogie hearth furnace, forging into a thick slab, slow cooling in heated bells, abrasive cleaning, heating of thick slabs in walking beam furnaces, rolling into 180-mm thick slabs, slow cooling in heated bells, and abrasive cleaning.

In a bid to reduce costs and decrease CO_2 emissions into the atmosphere, it was decided to cast this steel on a vertical continuous casting machine into slabs with thicknesses of 300 and 400 mm and widths of 2000–2500 mm. Experimental casting demonstrated that the slab surface was affected by such surface defects as "scabs," "longitudinal cracks along the scabs," and "flash" (failed breakthrough of the ingot crust) [1].

The depth of the defects did not allow for the slab to be cleaned to obtain a slab of the given thickness of 70–100 mm (see Figs. 1, 2 and 3).

Translated from *Metallurg*, No. 11, pp. 4–8, November, 2023. Russian DOI https://doi.org/10.52351/00260827_2023_11_4

https://doi.org/10.1007/s11015-024-01652-2 https://doi.org/10.1007/s11015-024-01652-2

Table 1 Chemical composition of steel

Parameter	Element content, wt. %					
	C	S	P	Si	Mn	Cr
Min	0.28	–	–	0.15	1.00	15.0
Average	0.33	–	–	0.20	1.10	16.0
Max	0.38	0.10	0.03	0.30	1.20	17.0

Additionally, the swing traces often had a curved shape, and a "slag inclusion" defect was detected, which indicates suboptimal operation of the slag on the metal meniscus in the mold. Visual observation as the slab entered the secondary cooling zone at 0.16–0.18 m/min operating casting speed revealed hot spots at the site of scab formation (see Fig. 4).

Three hypotheses were proposed to explain the causes of the formation of the defects:

- discrepancy between the mold settings and the actual shrinkage of the ingot crust.
- disruption of slag operation in the mold, resulting in an insufficient amount of slag entering some areas of the ingot crust.
- discrepancy between the calculated steel liquidus temperature and actual temperature.

Fig. 1 "Scabs" defect

Fig. 2 Defect: "cracks along the scab"

Fig. 3 "Flash" defect

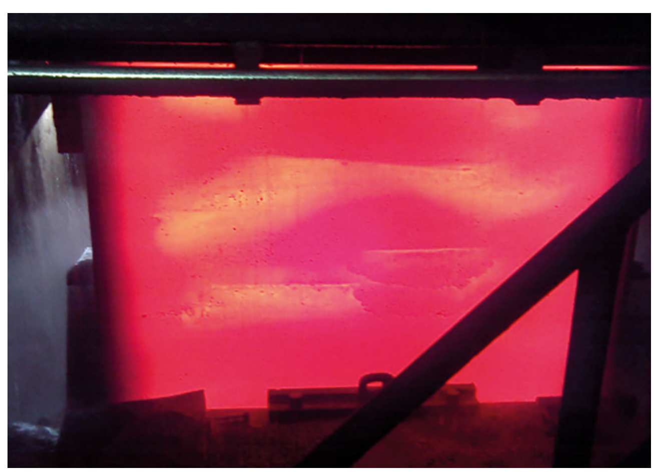

Fig. 4 Increased surface temperature in the ingot thinner crust area at the scab formation site

Observation of slag operation in the mold revealed that the slag evenly melts on the metal meniscus in the mold and does not accumulate in the form of unmelted parts; additionally, no flashes of metal are noted, and the amount of its consumption corresponds to the slag-forming mixture (SFM) certificate. Therefore, the main attention was paid to testing only hypotheses 1 and 3.

Optimization of mold tapering

The large amount of chromium and carbon in steel inhibits its high-temperature shrinkage (overall shrinkage increases) [2].

The high-temperature shrinkage of a steel sample was measured using an L78 RITA (Rapid Induction Thermal Analysis) dilatometer (see Fig. 5).

The high-temperature shrinkage of an ingot was calculated based on the combined solution of thermal and deformation problems [3–5].

The heat flow was assessed on the basis of the temperature at the outlet of the mold and the distribution of the heat flow for which the calculation was performed (see Fig. 6).

A mold with modified tapering of wide and narrow faces was developed on the basis of the ingot shrinkage calculations (Fig. 7).

To heat the meniscus, a closed-bottom submerged nozzle was used with an angle of inclination of the side holes of 10° upward (rather than 0°) and the shape of the outlet holes in the form of a keyhole, which further deflected the jet upward.

Two types of SFMs, *SRCP 417 SHR* and *SRCP 823 SHR*, were developed by Sheffield Hi-Tech Refractories.

The properties of *SFM SRCP 417 SHR* are as follows:

- Softening point: 1050 °C
- Temperature
  - melting: 1090 °C
  - Flow: 1110 °C
- $\eta_{1300\,°C} = 0.23$ Pa · s (values from measurements on a viscometer).

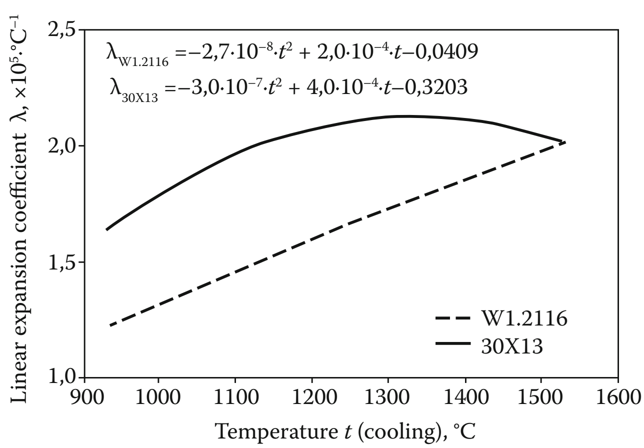

Fig. 5 Measurement of the high-temperature shrinkage of a steel sample

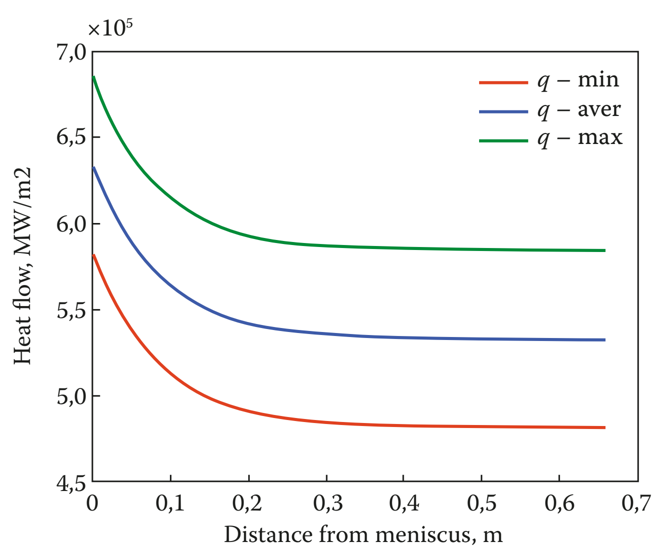

Fig. 6 Heat flow for which shrinkage was determined

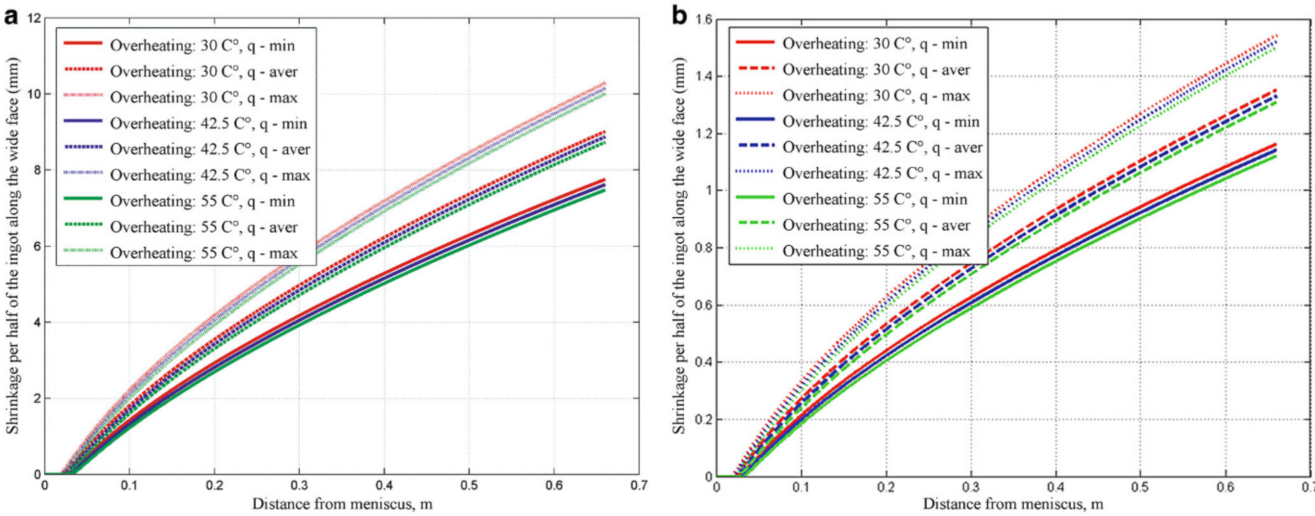

Fig. 7 Shrinkage of the ingot along the narrow (*a*) and wide (*b*) faces

The properties of *SFM SRCP 823 SHR* are as follows:

- Softening point: 870 °C
- Temperature:
  - melting: 1110 °C
  - Flow: 1120 °C
- Bulk density: 0.55 g/cm^3
- $\eta_{1300\,°C} = 0.33$ Pa · s (values from measurements on a viscometer).

The difference between the temperatures of the cooling water at the inlet and outlet of the mold was measured. It has been established that the scatter in the values of water temperature difference in the mold is more at higher temperature of metal in the tundish ladle in comparison with when the temperature decreases and the cooling conditions are stabilized. This confirms the hypothesis regarding the influence of metal overheating on the formation of the defects. Additionally, the spread of water temperature differences in the mold was smaller when using *SFM SRCP 417 SHR* than when using *SFM SRCP 823 SHR*.

Subsequently, casting was performed on *SFM SRCP 417 SHR* using a submerged nozzle with holes inclined upward by 10°.

The consistency of the polynomial for calculating the liquidus temperature of the steel was tested.

When casting slabs with defects, a well-known polynomial was used to calculate the liquidus temperature of the steel [6]

$$T_{\text{liq}} = 1536 - (78\text{C} + 7.6\text{Si} + 4.9\text{Mn} + 1.3\text{Cr} + 3.1\text{Ni} + 4.7\text{Cu} + 3.6\text{Al} + 34.4\text{P} + 38.0\text{S})\,.$$

A temperature calculation model was developed [7] (see Fig. 8) using literature data on modeling the liquidus temperature of steel based on the iron-chromium-carbon ternary diagram [8–20].

The following polynomial was developed:

$$T_{\text{liq}} = 1538 - (((78.43\text{C})_2 + (1.3913\text{Cr})_2)_{0.5} + 12\text{Si} + 6\text{Mn} + 3.1\text{Ni} + 4.7\text{Cu} + 28\text{P} + 30\text{S} + 2.53\text{Mo} + 0.35\text{W}).$$

The polynomial was tested by measuring the temperature and thermal characteristics of the steel samples using a simultaneous thermal analyzer (STA 449 F3 Jupiter, type S). The diagram is shown in Fig. 9. The liquidus temperature of the steel was in the range of 1480 °C–1490 °C.

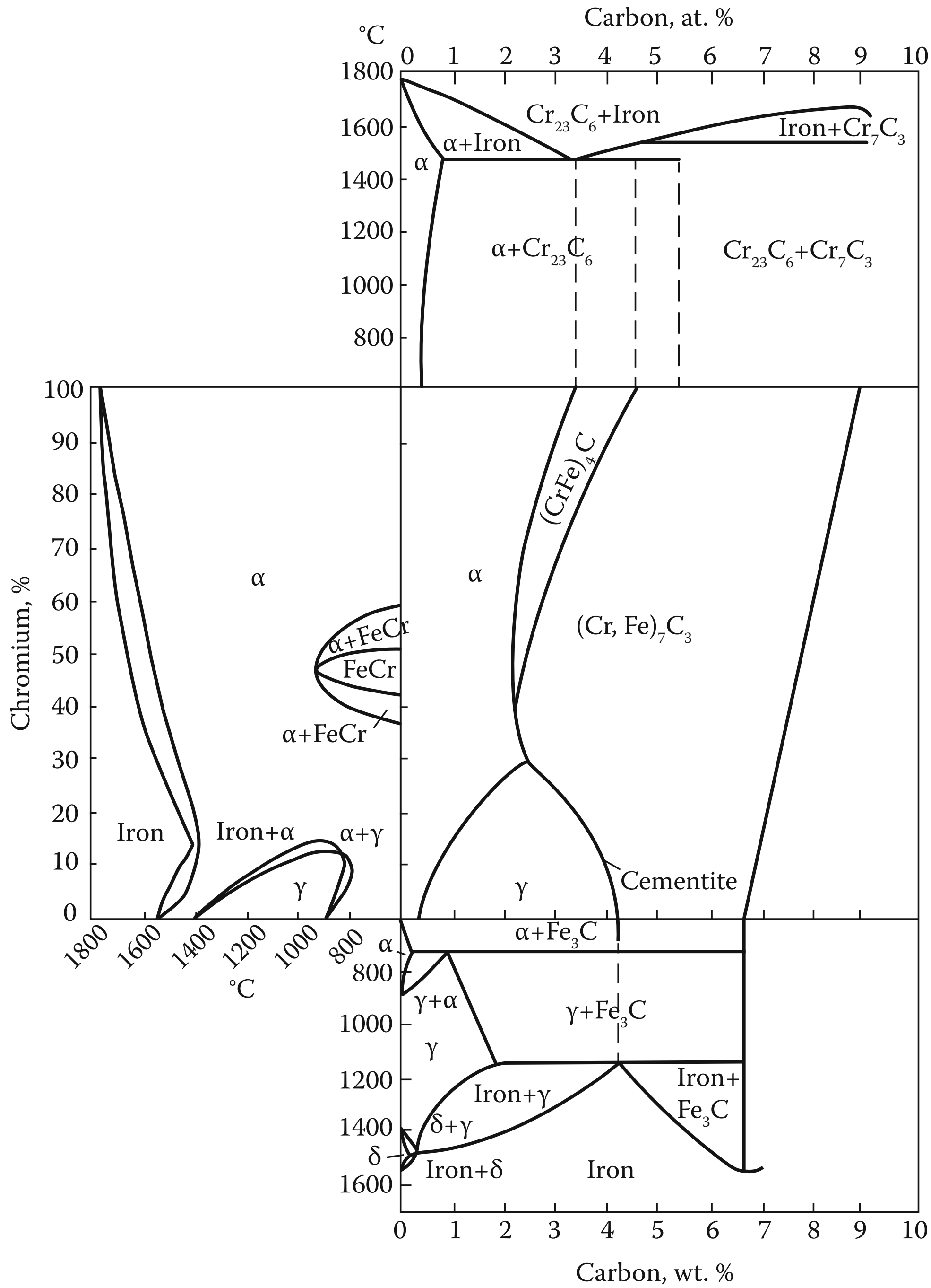

Fig. 8 Iron-chromium-carbon diagram [7]

Almost complete correspondence was observed between the calculated and measured liquidus temperatures. Using the developed polynomial enabled to avoid both excessive metal overheating, which leads to an uneven distribution of ingot crust temperature, and metal overcooling, which creates difficulty during casting and overcooling of slag surface in the mold. The temperature and speed conditions for steel casting were adjusted on the basis of the calculation results as follows:

Overheating of steel in the tundish ladle, °C	Ingot drawing speed, m/min
Less than 45	0.17
46–50	0.16
51–55	0.15

Fig. 9 Diagram from STA 449 F3 Jupiter, type S

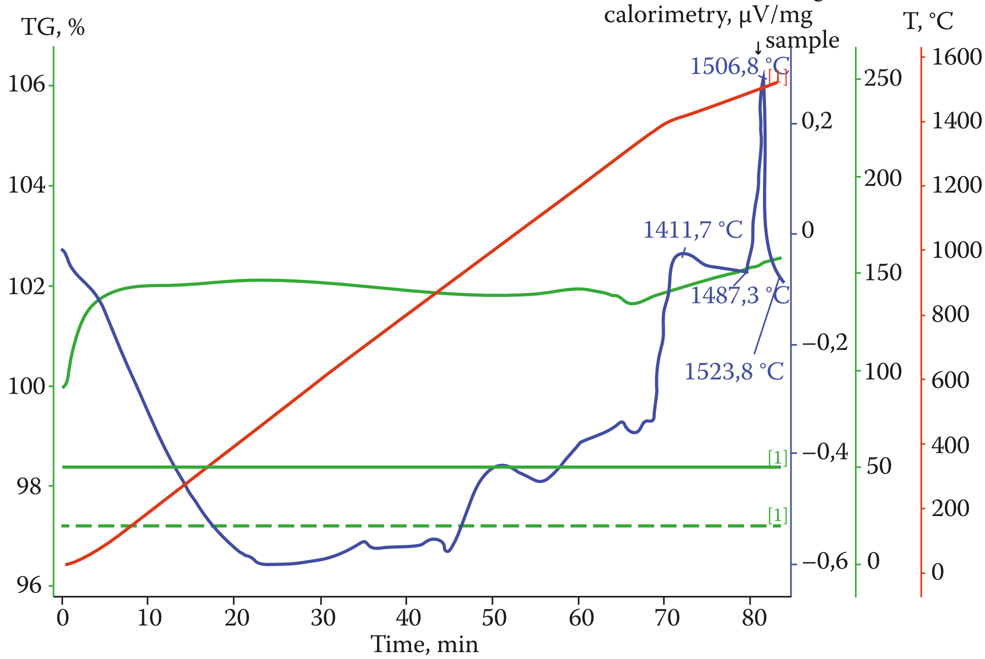

Fig. 10 Surface of 400-mm-thick slabs cast after introducing the technology

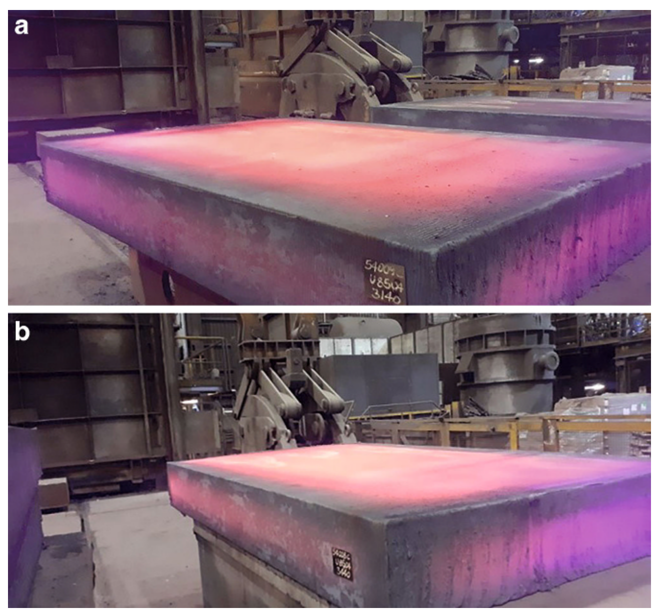

Conclusions

Slabs with considerably improved quality (see Fig. 10) were obtained using the developed measures in the form of a new polynomial for calculating the liquidus temperature of the steel, new temperature-speed modes of casting, new settings (tapering) of the mold, and optimization of immersion nozzle design and SFM composition:

1. Surface defects such as "scabs," "longitudinal cracks along the scabs," and "flash" were avoided.
2. This allowed for hot loading of slabs into a walking beam furnace and considerably reduced abrasive cleaning of the intermediate roll surface.
3. The narrow edge became flatter, and more even traces of the mold swing appeared on it.

References

1. Botnikov SA (2011) A modern atlas of defects in continuous cast billets and the causes of defects in breakthroughs of the crystallizing crust of the metal. Volgograd
2. Kuklev AV, Leites AV (2011) Practice of continuous casting of steel. Metallurgizdat, Moscow
3. Kabakov ZK, Gabelaya DI (2001) Study of ingot shrinkage in a mold during continuous steel casting, progressive processes and equipment for metallurgical production, proceedings of II all-Russian scientific-technical conf. ChSU Cherepovets: 53–55
4. Gabelaya DI, Kabakov ZK, Gribkova YV (2016) Mathematical models and improvement of continuous steel casting technology. ChGU Cherepovets
5. Kabakov ZK, Gabelaya DI (2000) Mathematical model of solidification and cooling of a continuous rectangular ingot, increasing the efficiency of heat transfer processes and systems, proceedings of II international scientific-technical conf. VoGTU Vologda: 131–133
6. Niskovskikh VM, Karlinsky SE, Berenov AD (1991) Continuous casting machines for slabs. Metallurgiya, Moscow
7. Berezovskaya VV, Ishina EA, Ozerets NN (2016) Diagrams of the state of ternary systems. Izdatel'stvo Uralskogo universiteta, Yekaterinburg
8. Smirnov AN, Nedelkovich L, Dzhurzhevich D, Chernobaeva TV, Odanovich Z (1996) Calculation of the liquidus temperature of steel. Stal (3):15–19
9. Kabishov SM, Trusova IA, Ratnikov PE, Korneev SV (2015) Determination of the boundaries of the two-phase zone of carbon and alloy steels. Lit'ye Met (2):82–88
10. Kawakami K, Kitagawa T, Miyashita Y et al (1982) Nippon Kokan technical report. Overseas 36:26–27
11. Deuxieme Conf. Mondial des Founders a models perdus (Dusseldorf, 1–4 June, 1960).
12. Aymard JP, Detrez P (1974) Fouderie. Janvier 330:11–24
13. Hirai M, Kanamru K, Mori H (1969) Tetsu To Hagane 52:85
14. Roeser WR, Wensel HT (1941) Freezing temperatures of high-purity iron and some steels. J Res Natl Bur Stand 26:273–287
15. Kagava A, Okamota T (1986) Influence of alloying elements on temperature and composition for peritectic reaction in plain carbon steel. Mater Sci Technol 2(10):997–1008
16. Andrews KW (1981) Solidification ranges of steel. A Note Submitt To Alloy -ph Diagr Date Comm Met Soc: 1–8
17. Wolf M (1982) Zurich, pp 37–49
18. Howe AA (1988) Estimation of liquidus temperatures for steels. Ironmak Steelmak 16(3):134–142
19. Schiirmann E, Schweinichen JV, Volker R (1987) Giesserei-Forschung 39. Jahrgang (4):133–136
20. Sugden A, Bhadeshia H (1989) Thermodynamic estimation of liquidus, solidus Ae 3 temperatures, and phase compositions for low alloy multicomponent steels. Mater Sci Technol 5(10):977–984. https://doi.org/10.1179/mst.1989.5.10.977

Authors and Affiliations

✉ A. V. Kuklev
a.kuklev@chermet.net

V. V. Tinyakov
tvv@corad.ru

A. V. Ermolaev

C. Zamboni
c.zamboni@eu.nlmk.com

E. Donskoi
evgeni.donskoi@sheffield-refractories.de

A. V. Kuklev, V. V. Tinyakov
I.P. Bardin TsNIIChermet, Moscow, Russian Federation

A. V. Ermolaev, C. Zamboni
NLMK-Verona, Verona, Italy

E. Donskoi
Sheffield Hi-Tech Refractories, Emmerich am Rhein, Germany